[1]Biqing Li
[1,*]Shiyong Zheng
[2]XiaoguangYue

A MIMO-Based Dual Polarized Antenna Applicable for Mobile Terminal

Journal of Electrical Systems

Abstract: - At present, numerous small-size mobile terminal devices, such as mobile phones, have embedded the antenna in the cases, which will lead to considerable restrictions on the space for installing multiple antennas. Aiming at the requirements of rational design and layout of multi-antennas for MIMO mobile terminals and combining with the broadband and miniaturization technologies, a dual polarized antenna suitable for mobile terminals was designed in this paper through an adoption of polarization diversity. For a dual polarized multilayered micro-strip antenna with a ground plate, it is easy to be conformal to the carrier. In this paper, the design and the process of simulation optimization of the antenna unit were analyzed in detail. The bandwidth of the antenna unit was 1890 to 2200 MHz, the return loss was superior to -33dB, and both of the horizontal polarization gain and the vertical polarization gain were 8.2 dB. Accordingly, the characteristics of a high gain and dual polarization were achieved.

Keywords:Multiple antennas of mobile terminals; Broadband; Miniaturization technologies.

I. INTRODUCTION

Targeting at the features of the mobile terminal devices themselves, the following design requirements related to the multiple antennas of the MIMO system mobile terminals can be obtained:

(1) In order to obtain the diversity gain, the multi-antenna layout of the mobile terminals needs to use a combination of diversity methods;

(2) In order to enable the antenna to have as wide a lobe as possible in the forward direction while to have as small a radiation as possible in the backward antenna so as to reduce the SAR of the antenna, the orientation pattern of the antenna unit is required to be optimized;

(3) A dual polarization and even multiple polarization ought to be realized;

(4) An appropriate measure should be adopted to drop down the volume of the antenna unit, and accordingly, a miniaturization design would come true.

In regard to the micro-strip antenna, a linear polarization of two-path orthogonality is completely able to be realized on the same patch if a proper feed position has been chosen under the condition where there is no need of an additional increase in the volume of the antenna. Moreover, at the same time of a selection among the diversity modes for the multiple antennas of MIMO mobile terminals, a polarized diversity is generally selected so that we can couple with the special properties of the micro-strip antenna to put the design of dual polarization into to realization.

For the purposes of an improvement in thediversity gain and a decrease in the adverse effects on the systems due to the failure of pairing of the antenna polarization, we are supposed to select out a suitable technical program when the antennas for the MIMO-system mobile terminals are in designing, so as to reach the dual polarization design of the antennas.

II. DESIGN OF THE ANTENNA UNIT

Due to the small volume of the mobile terminal devices themselves, the requirements for the multiple antenna design of the mobile terminals are very strict. Based on such a situation, various requirements for the antennas are correspondingly came up with, that the antenna is supposed to be small in the size, low in the cross section, light in the weight, diversifying in the electrical properties, easy conformity with the carrier, and conducive to be an integration with active devices and circuits as a unified component. In view of the above requirements for multi-antenna design of mobile terminals in MIMO systems, two different types of antenna elements have been designed in this chapter, one of which is a dual-polarization multilayered micro-strip antenna with a structure of double-layer dielectric plate, and the other is a slot-shaped dual polarization antenna. In addition, the effects of the main parameters of the antenna unit structure on the S-parameters of the antenna elements have been analyzed in detail, respectively. The overall idea of designing the antenna unit followed the following pattern. First of all, the technical indicators that need to be achieved were combined with the antenna structure initially

[1,*]School of Business, Guilin university of electronic technology, Guilin,Guangxi , China
[2]Wenzhou Business College, Wenzhou 325035, China

determined. Through an analysis and calculation with the classical theory of the antenna, the parameters of the structure of each part of the antenna unit were and obtained. Then, these parameters were brought into the simulation software for the establishment of a model on the antenna. The last step was to compare these technical indicators with the simulation results, and to modify these parameters of the antenna structure repeatedly until the simulation results met the required technical indicators.

The dual-polarized multilayered micro-strip antenna and the slot-shaped dual-polarized antenna studied in this paper were both applied to the mobile terminal equipment with the GSM band and CDMA band. The main design indicators of the antenna were: The working band was 1.9 to 2.2 GHz; the return loss was≤-10dB; and the bandwidth≥300MHz.

A. Analysis of the Antenna Parameters

In the designing of a micro-strip antenna, how to select the dielectric substrate of the antenna is a process of importance. The dielectric constants ε_r and $\tan\delta$ of the dielectric substrate and the thickness h of the dielectric substrate are all the parameters that directly affect the performance of various aspects of the micro-strip antenna. In addition, the size of the antenna patch, the bandwidth of the antenna, the accuracy of the physical production, and the impedance of the feeder line can also affect the performance of the micro-strip antenna. For these causes, in the actual production of the antenna body should be based on the specific needs of the various parameters of the antenna to be weighed.

For the effective utility of space, a dielectric substrate with relatively low ε_r is generally used in designing the micro-strip antenna. If a lower resonant frequency is in demand, the dielectric substrate with a high ε_r can be taken into consideration. Besides, on the premise that the dielectric constant is kept unchanged, a dielectric substrate with a large thickness is allowable to be selected if a large bandwidth is to be obtained. However, the dielectric substrate with a large thickness will increase the surface wave of the patch. Assuming that the operating frequency of the antenna is f , and the formation of the surface waves need to be avoided, the thickness h of the dielectric substrate should satisfy the following equation :

$$h \le \frac{0.3c}{2\pi f\sqrt{\varepsilon_r}} \quad (1)$$

From the above equation, it can be known that the input impedance will increase with the increase of the dielectric constant, and the port isolation will also increase under the condition where the thickness of the dielectric substrate is kept constant. With the dielectric constant remaining constant, the elevation in the substrate thickness can reduce the input impedance and the isolation will also be dropped down at the same time.

Since that these parameters of the volume, isolation and bandwidth of the antenna are mutually restrictive, a balanced consideration ought to be applied according to the actual design requirements in the antenna design process, and thus suitable materials will be selected. In addition, the machinability of the dielectric substrate is also in need of being taken into consideration, and the material for the antenna is preferably prevented from being affected by environmental factors such as temperature and humidity. Hereby, the dielectric substrate selected in this paper is Fb4-1, with a dielectric constant ε_r of 2.65, $\tan\delta$ =0.0005. and the thickness h of 1mm.

Under general circumstances, the basic size of the antenna is mostly obtained from a rough calculation with the empirical formula first in the designing of the micro-strip patch antenna.

The formula for the determination of the width W of the antenna unit is:

$$W = \frac{c}{2f_r}\left(\frac{\varepsilon_r + 1}{2}\right)^{-\frac{1}{2}} \quad (2)$$

In this formula, c is the speed of light, f_r is the resonant frequency, and ε_r is the dielectric constant of the dielectric substrate. The length L of the micro-strip patch antenna element is generally approximately equal to $\lambda_g / 2$; however, in the fact that it will be influenced by the fringe field, the size L of in the actual design should be subtracted by $2\Delta L$ from $\lambda_g / 2$. Here, the value of ΔL is given by the equation below:

$$\frac{\Delta l}{h} = 0.412\frac{(\varepsilon_e + 0.3)(W/h + 0.264)}{(\varepsilon_e - 0.258)(W/h + 0.8)} \quad (3)$$

Wherein, h is the selected thickness of the dielectric substrate, and ε_e is the effective dielectric constant of the dielectric substrate. ε_e can be expressed as:

$$\varepsilon_e = \frac{\varepsilon_r + 1}{2} + \frac{\varepsilon_r - 1}{2}(1 + \frac{10h}{W})^{-\frac{1}{2}} \quad (4)$$

The length L of the antenna unit can be expressed by the equation below:

$$L = 0.5\lambda_g - 2\Delta L \quad (5)$$

Wherein, λ_g is the dielectric wavelength, which can be obtained through the calculation from $\lambda_g = \lambda_0 / \sqrt{\varepsilon_e}$ (λ_0 is the wavelength of free space).

Or, the length L of the antenna unit can be expressed by the equation below:

$$L = \frac{c}{2 f_r \sqrt{\varepsilon_e}} - 2\Delta L \quad (6)$$

In general situations, the size of the dielectric substrate is the one that is widened outward at $\lambda_g / 10$ along the sides of the radiating element.

According to the formula above, it can be seen that the value of L is closely related to ε_r. After the L and W are given, the size and weight of the antenna will be determined by h. When ε_r and h are known, the selected value of ε_e is determined by W, while the selected value of W will pose an impact on the directivity function, the input impedance, and the radiation resistance of the micro-strip antenna, which in succession will influence the radiation efficiency and bandwidth of the antenna. Additionally, the selected value of W directly dominates the size of the micro-strip antenna; the larger bandwidth is beneficial to the frequency band, impedance matching, and efficiency if the mounting space permits. In contrary, when the W is too large, high-order modes will occur, causing a distortion of the field.

B. Design of Dual-polarized Multilayer Micro-Strip Antenna Unit

Through the comparisons between various antenna types, it can be found that he dual-polarization micro-strip antenna occupies more potential for miniaturization than that for the single-polarization micro-strip antenna; furthermore, it is easy for the micro-strip antenna with the ground plate to be conformal with the carrier. Currently, the mobile terminal devices gradually form a design trend of embedding an antenna into the cases of the devices. For this end, a design was conducted on the adopted dual polarization micro-strip antenna with a ground plate in this program. And the detailed analysis on the process of designing the antenna unit is as follows.

(1) Analysis of Antenna Unit Structure

The structure of the antenna unit is shown as in Figure 3.1. The antenna uses a multi-layer structure to increase the effective dielectric height of the antenna and introduces an air layer to broaden the frequency band. The antenna unit adopts a rectangular radiation patch, and a preliminary calculation based on empirical formula (2) yields w=55.5mm. After an optimization simulation with the CST MICROWAVE STUDIO electromagnetic simulation software based on finite integral method, the obtained size of the antenna radiation patch is 53mm.

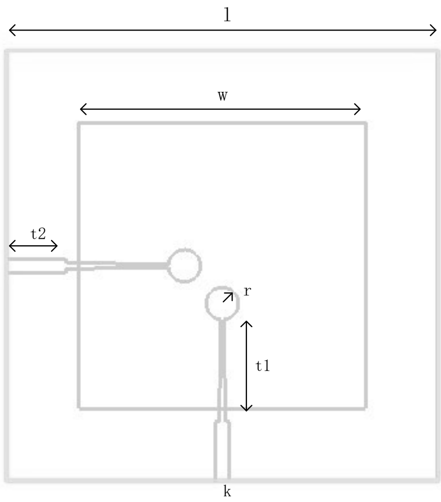

Fig. 1. Diagram of the unit structure --Structure diagram of double-polarized multilayer micro-strip antenna

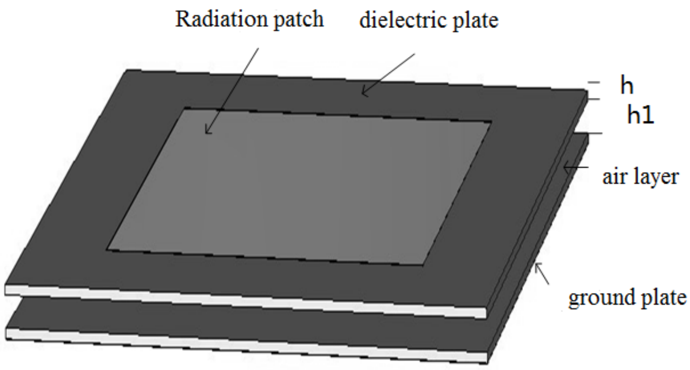

Fig. 2. Stereogram of the unit--Structure diagram of double-polarized multilayer micro-strip antenna

The description of each parameter are as follows: The width of the two dielectric plates is l, the thickness is h, and the dielectric constant is 2.65. w is the width of the rectangular radiating patch. Adjusting the value of w allows the resonant frequency to be adjusted to the desired operating frequency. The height of the air layer is h1. The feeder line is placed on the back of the first layer of media board and can be divided into three parts. The front end adopts a wafer with radius r, which makes the matching easier to adjust. The middle part is a matching branch section, and the length is t1. A gradient line structure is adopted, and the gradual adjustment amplitude can be used to make the frequency band be broadened, and a better matching can be achieved accordingly. The back-end part is a 50ohm matching feeder line, with the length of t2 and the width of k.

III. Optimization simulation of antenna unit

This program used the CST MICROWAVE STUDIO electromagnetic simulation software based on the finite integral method for analysis. Firstly, a simulation software was applied to set up an antenna model, and then the waveguide port of 50 Ω was chosen to serve as the input port of the antenna. Soon after that, an adjustment was performed on the size of the antenna. The simulated value of the reflection loss was used to determine the optimal antenna unit structure size. Next, the influence of the main parameters of the dual-polarized multilayer micro-strip antenna structure in Figure 3.1 on the S-parameters of the antenna was discussed.

A. The width of the radiation patch w was adjusted

The width of the radiation patch w was adjusted, and the change of the parameter S is shown in Figure 3.2, where the adjusting values were 47mm, 50mm, 53mm, 56mm, and 59mm, respectively.

Adjusting the value of w, both of the curve changes of S11 and S12 were obvious. From the Figure (a), it can be seen that the resonant frequency of the 1 port gradually becomes smaller as the w value gradually increased, the bandwidth of the port was basically kept at about 300 MHz; and its return loss also changed; first it became larger as w increased and the best result was obtained at w=53mm; and then it became smaller as the value of w continued to increase. The change rule of the S22 curve in Fig. (b) was basically the same as that of the S11 curve, and the change law of the port resonance frequency and the bandwidth is basically the same as that of the change of port 1. As can be seen from (c), the curve of the isolation of the two ports S21 also gradually shifted to the left as the value of w changes, and basically moved as the resonant frequencies of the two ports move. Although all of them could reach -15dB in the bandwidth range, the result was still not satisfactory. After comparing the curve changes of the S-parameters, the resonance frequency, return loss, and bandwidth of the two ports and the isolation of the two ports were taken into consideration. Finally, w=53 mm was selected.

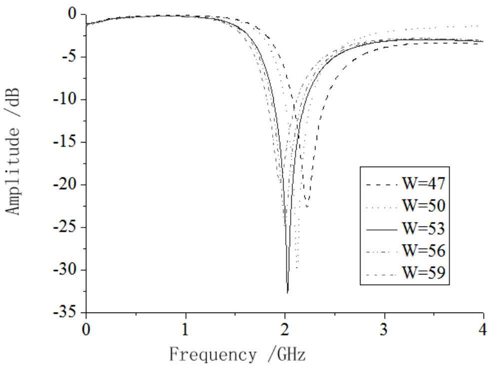

Fig. 3. The Changing curve of S parameter with adjusting the value of w--Changing curve of S11

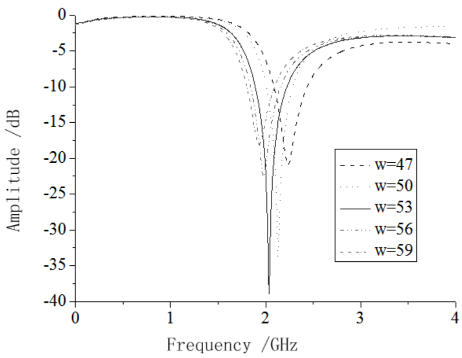

Fig. 4. The Changing curve of S parameter with adjusting the value of w--Changing curve of S22

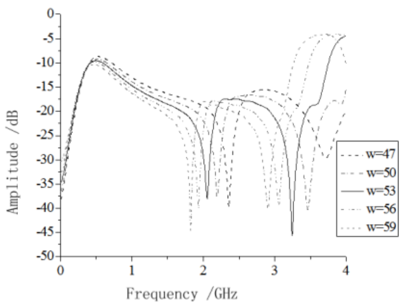

Fig. 5. The Changing curve of S parameter with adjusting the value of w--Changing curve of S21

B. The matching stub length t1 of the feeder line were adjusted

The matching stub length t1 of the feeder line were adjusted and the changing state of S parameter was shown in Figure 3.3, where the adjusting values were 13mm, 16mm, 19mm, 22mm, and 25mm, respectively.

Adjusting the value of t1, both of the curve changes of S11 and S12 were obvious. It can be seen from the figure (a) that when the value of t1 gradually increased, the resonant frequency of the 1 port also changed, fluctuating around the center of the value obtained at t1=19mm. The port bandwidth was basically kept at 300

MHz, and the return loss value remains substantially below -30dB. The S22 curve in Figure (b) also varied with the value of t1. The resonance frequency swing of the 2 port is obvious. The port bandwidth and return loss of the port were similar to those of the 1 port. From the figure (c), it can be seen that the curve of the two-port isolation S21 did not show a large change, and both can reach -15dB in the bandwidth range. Finally, a comprehensive consideration on the resonance frequency, return loss and bandwidth of the two ports was performed, and the t1=19mm was selected, which can make the resonant frequencies of the two ports most similar to each other.

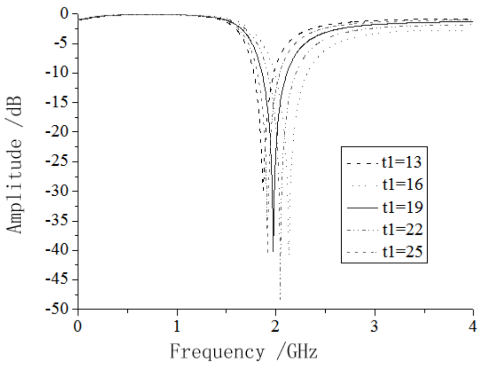

Fig. 6. The Changing curve of S parameter with adjusting the value of t1-- Changing curve of S11

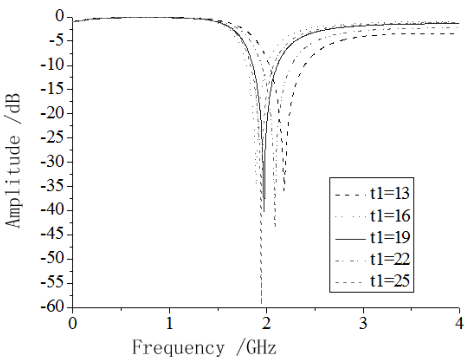

Fig. 7. The Changing curve of S parameter with adjusting the value of t1-- Changing curve of S22

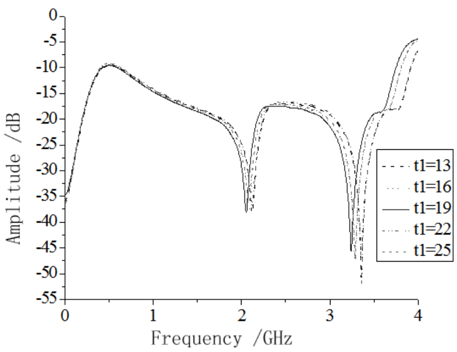

Fig. 8. The Changing curve of S parameter with adjusting the value of t1-- Changing curve of S21

C. The portslength t2 of the feeder line were adjusted

Adjusting the portslengthof t2, both of the curve changes of S11 and S12 were obvious, where the adjusting values were 7mm, 9mm, 11mm, 13mm, and 15mm, respectively.

Adjusting the value of t2 will mainly affect the return loss of the two ports. From Figure (a), it can be seen that when the value of t2 gradually increased, the return loss of port 1 first increased; then, it reached the maximum at t2 = 11 mm and after that it gradually became smaller; its resonant frequency does not change significantly and basically was maintained at the position of 2GHz. Similarly, the port bandwidth did not present a significant change and it was remained at around 300MHz. The variation of the S22 curve in Figure (b) was basically the same as that of the S11. The port resonant frequency and the change of the bandwidth and the return loss were basically the same as those of the port 1. From the figure (c), it can be seen that the curve of the two-port isolation S21 did not change greatly and both can reach -15dB in the bandwidth range. After a comprehensive consideration on the resonance frequency, return loss and bandwidth of the two ports was performed, and the t2=11mm was selected with which a generally good result was obtained.

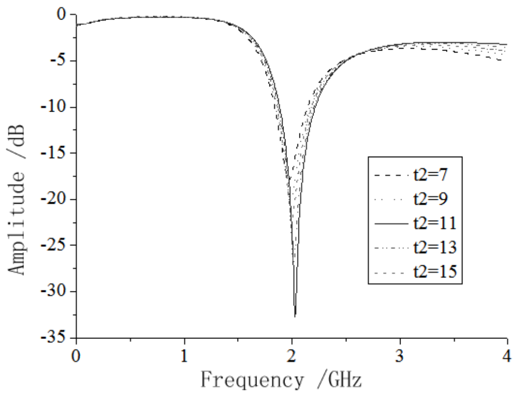

Fig. 9. The Changing curve of S parameter with adjusting the value of t2--Changing curve of S11

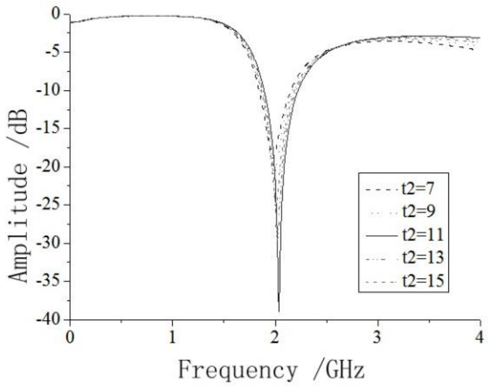

Fig. 10. The Changing curve of S parameter with adjusting the value of t2--Changing curve of S22

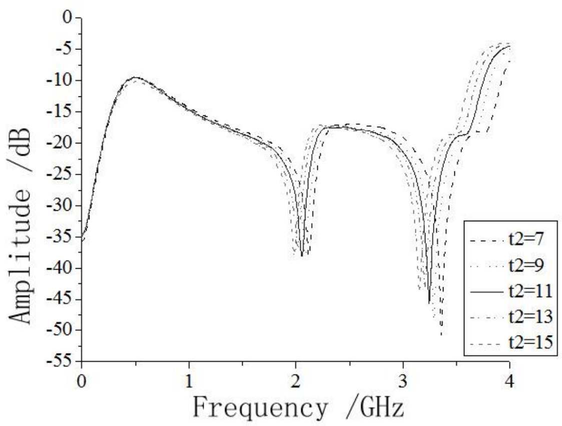

Fig. 11. The Changing curve of S parameter with adjusting the value of t2--Changing curve of S21

Through the scanning and optimization of the above main parameters, the parameters of the antenna can be determined finally, and it can be concluded that the reflection coefficients S11 and S22 of the two ports of the antenna had a bandwidth range of 1890 to 2200 MHz at -10dB. The center frequencies of the two ports of the antenna coincided. At the center frequency, S11 was -33dB and S22 was -38dB. The two-port isolation S21 can reach -15dB over the entire operating band. The antenna had a working bandwidth of 310 MHz, covered the GSM band and the CDMA band, and met the design requirements for an antenna bandwidth of ⩾300MHz. The optimized S-parameter curve was shown in Figure 3.5. The final debugging parameters were shown in Table 3.1.

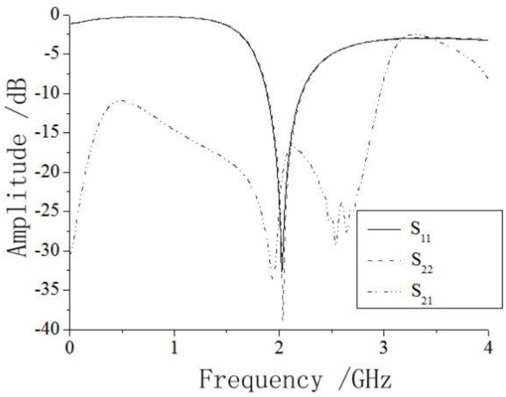

Fig. 12. Simulation values of S parameter after the optimization

Table 1. Values of each parameter (Unit: mm)

1	w	h	h1
70	53	1	2.2
r	t1	t2	k
3	19	11	2.7

The optimized antenna pattern simulation results are shown in Figure 3.6. Figure (a) shows the patterns of E-plane and H-plane of the 1-port, where the half-power beam-width of the E-plane is 73.2°, the half-power beam-width of the H-plane is 81.6°, the first side-lobe level is lower than -17.3dB, and the maximum gain reaches 8.2dB. Figure (b) shows the patterns of E-plane and H-plane of the 2-port, where the half-power beam-width of the E-plane is 73.1°, the half-power beam-width of the H-plane is 81.5°, the first side-lobe level is lower than -17.2dB, and the maximum gain reaches 8.2dB.

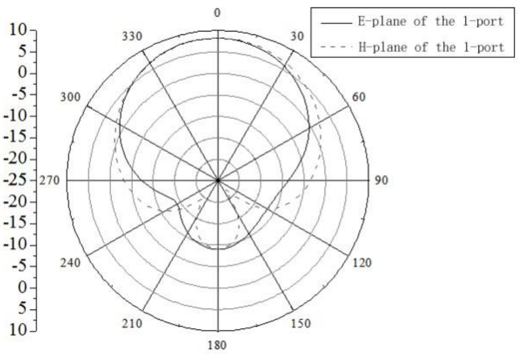

Fig. 13. The Simulation results of direction diagram after the optimization--Patterns of E-plane and H-plane of the 1-port

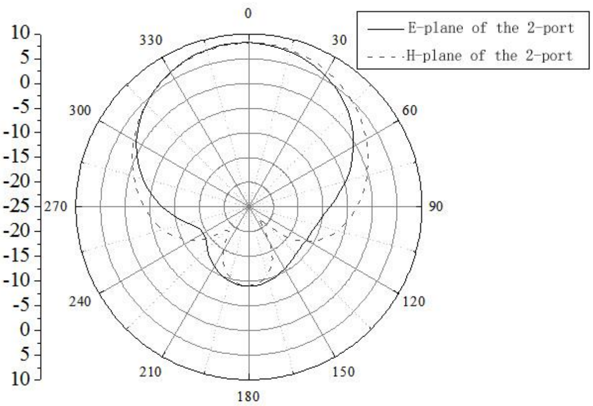

Fig. 14. The Simulation results of direction diagram after the optimization--Patterns of E-plane and H-plane of the 2-port

The above simulation results indicated that the dual-polarized multilayered micro-strip antenna unit can effectively realize the characteristics of wideband, high gain, and easy conformity, and it was easy for it to achieve the index requirements of the antenna design in this paper.

IV. CONCLUSION

At presently, the mobile communications are in a rapid development, while the spectrum resources demonstrate an increasing scarcity. To achieve a communication system with high speed and large capacity on the limited spectrum resources, the technology featured in an extremely-high efficiency of spectrum utilization is required. Fortunately, the MIMO technology is emerged accordingly in this situation. The communication system using MIMO technology is called MIMO communication system. Multiple antennas (or array antennas) and multiple channels are adopted at the transmitter and receiver, and their system capacity increases linearly with the increase of the minimum number of antennas at the transmitter and receiver. It is this significant feature that the popularity of MIMO technology has become one of the research hotspots in the field of wireless communications. Currently, the researches on the antenna in the MIMO system mainly focus on the antenna form, multiple antenna layout, and mutual coupling analysis. Since that the current communication products, especially mobile terminal devices, are moving toward miniaturization, the space for installing multiple antennas is considerably limited due to the small size of the equipment. Under this background, focusing on the design and layout requirements of multiple antennas for mobile terminals, a related research was performed in this paper.

Based on the analysis on the design requirements and technical approaches of the multi-antennas for MIMO mobile terminals in this paper, a small-size wideband antenna was created, which was designed to be a dual-polarization multilayer micro-strip antenna. This antenna adopted a double-layer dielectric plate structure, introduced an air layer, and the feeder was placed on the back of the first layer of the dielectric plate. The method of slotting the ground plate was failed to application so that the antenna structure was relatively simple. In this paper, a professional electromagnetic simulation software was used to analyze the design and simulation optimization process of the antenna unit in detail. And the results suggested that the working bandwidth of the dual-polarized multilayer micro-strip antenna was 1890~2200MHz, and the return loss was superior to the value of -33dB. Depending on these results, it can be known that the antenna operating bandwidth was 310 MHz which can cover the GSM band and the CDMA band, and the design requirements for the antenna bandwidth ⩾ 300 MHz have been achieved.

V. ACKNOWLEDGMENT

This work is supported the following fund:

2015 special topic of education informatization work of Guangxi Education Science 12th Five-Year plan :” Research on training monitoring and evaluation of Information technology capability upgrading project in Primary and secondary schools in Guangxi”(No, 2015zky25)

2016 Guangxi higher education undergraduate teaching reform project:” Reform and practice of integrated teaching mode based on mixed workshop “(No, 2016JGA404)

2017 The student work subject program of Hezhouuniversity:”college students' network addiction of the student work service research”(No,hzxysz201707).

2016 The higher education research subject project project of Hezhouuniversity:”between collaborative innovation research of entrepreneurial talent cultivation system”.

2017 college students' innovative entrepreneurial project:”The agricultural robot autonomous operations research based on machine vision”(No,201711838096)&&”Multi-functional autonomous agriculture robot development”(No,201711838121).

2017 Guangxi education science 'ten-three-five' planning project:”Based on zte's ICT education platform of fusion, work-integrated learning education training mode research”(No,2017B107).

2018 Project of improving basic ability of Young and Middle-aged Teachers in Guangxi Universities: ”design and implementation of picking Robot based on Internet of things”(No,2018KY0556).

REFERENCE

[1] B.Q LI, Y.F LING, M TIAN, S.Y ZHENG: Design and implementation of sugarcane growth monitoring system based on RFID and ZigBee. International Journal of Online Engineering, 3(14),134, (2018).

[2] B.Q LI, M TIAN, S.Y ZHENG,Y.F LING : Design and research of picking manipulator obstacle avoidance system based on IOT. International Journal of Online Engineering, 3(14), 96, (2018).

[3] B.Q LI, Y.F LING, H.Y ZHANG, S.Y ZHENG: The Design and Realization of Cherry Tomato Harvesting Robot Based on IOT. International Journal of Online Engineering, 12(12), 23, (2016).

[4] B.Q LI, W.L GUAN, S.Y Zheng, X.G Yue: OPTIMISATION DESIGN OF CORN PRECISION SEEDER BASED ON MULTI-ROUTE AND MULTI-CHANNEL CONTROL. Journal of The Balkan Tribological Association, 21(4A), 1215, (2015).

[5] U.A. SHAABAN,M.T.AFIFY,G.E. HASSAN,Z.A. EL-HADDAD:Development of aVacuum Precision Seeder Prototype for Onion Seeds. Misr J. Ag. Eng, 26(4), 1751, (2009).

[6] B.Q LI, X.M YANG GUAN, S.Y ZHENG : Internet of Things-based Simulation Study on Lijiang River Water Environment Monitoring. Journal of Coastal Research,79, 1-5, (2017).

[7] Y.A.SHAABAN: Development of an Appropriate Pneumatic Planter for Small Holding in Egypt. Colg Agric, Bha Uni, 46(8), 1999,(2010).

[8] P. K. AGARWAL, J. BASCH, L. J. GUIBAS, J. HERSHBERGER, L. ZHANG: Deformable Free Space Tiling for Kinetic Collision Detection. Proc. 4th WspAlgFd. Rbt, 54(3), 245,(2000).

[9] P. K. AGARWAL, J. ERICKSON, L. J. GUIBAS: Kinetic Binary Space Partitions for Intersecting Segments AndDisjoint Triangles. Proc. 9th ACM-SIAM ,44(6), 578,(1998).

[10] Z.B. BARUT, A. OZMERZI: Effect of Different Operating Parameters on Seed Holding in the Single Seed Metering Unit of a Pneumatic Planter. Turk. J. Agric, 28, 435, (2004).

[11] M. J. ATALLAH: Some Dynamic Computational Geometry Problems. Comp. Math. Appl, 11(12), 1171 (1985).

[12] J. BARRAQUAND, J. C. LATOMBE: Robot Motion Planning: A Distributed Representation Approach. Int. J. Rbt. Res, 10, 628, (1991).

[13] M. BERN, P. PLASSMANN: Mesh generation. In J.-R. Sack and J. Urrutia, editors, Handbook of Computational Geometry. Els Sci Pub B.V.Ams, 16(4), 566,(2000).

[14] A. VASS-VARNAI, R. BORNOFF: Thermal Simulations and Measurements – a Combined Approach for Package Characterization. ICEP, Jpn,76(4), 886,(2000).

[15] V. THIYAGARAJAN, K. KALAICHELVAN, K.SRINIVASAN,S. VENUGOPAL, R. VIJAY: Influence of Specific Heat Capacity on Hybrid Non-asbestos Brake Pad Formulation. J. Balkan Tribol. Asc, 10(8), 102, (2015).

[16] L. YANG, X.T. HE, T. CUI, D. X. ZHANG, S. SHI, R. ZHANG, W. MANTAO: Development of Mechatronic Driving System ForSeed Meters Equipped on Conventional Precision Corn Planter. Int J Agric & Biol Eng, 8(4), 1, (2015).

[17] D. KARAYEL, Z.B. BARUT, A. OZMERZI: Mathematical Modeling of

[18] Vacuum Pressure on a Precision Seeder. Byst. Eng, 87(4), 437, (2004).

[19] X.G. YUE, G. ZHANG, Q. WU, F. LI, X.F. CHEN, G.F. REN, M. LI: Wearing Prediction of StelliteAlloys Based on Opposite Degree Algorithm. Rare Metals, 34(4), 125, (2015).

[20] Z. ZONGMING: Research on Wearing Prediction of the Cylinder Surface Based on Time Series Autoregressive (AR) Model. ICMTMA, Hong Kong, 12(1), 960, (2013).

[21] S. SPINU: Numerical Simulation of Viscoelastic Contacts. Part 1. Algorithm Overview. J. Balkan Tribol. Assoc, 10(5), 269, (2015).

1 Authors

LI BIQING (1984-),come from Nanning, Guangxi province. master degree, senior engineer , the main research direction for broadband MINO, IOT,Big data analysis.(e-mail: 318281853@ qq.com).

ZHENG SHIYONG (1983-), come from Guilin, Guangxi province. PhD , senior engineer , the main research direction for network marketing, IOT.(e-mail: 29291838@ qq.com).